Measurement of the branching fractions of $B^0_{(s)} \to K^0_S hh'$ at LHCb and sensitivity study of $B^0 \to K^{*0}\tau^+\tau^-$ at FCC-ee

Tristan Miralles - LPC (Clermont-Ferrand)
tristan.miralles@clermont.in2p3.fr

JRJC Saint-Jean-de-Monts - 23th of October

Motivations

- **Standard Model** (SM) describe the **small scale process** with an **incredible precision**.
- **SM include** *CP* **violation**.
- **But not enough** to explain the **amplitude of the matter-antimatter asymmetry** in the universe.
- **One goal of Flavour Physics** : ~~understand the taste of the préfou~~ **discover other sources of** *CP* **violations** to enhance the SM.
- $B-$**mesons** $|b\bar{q}' >$ **decays** by including bottom quark ($m_b = 4.18\,\mathrm{GeV}/c^2$) transitions are **laboratories to study** *CP* **violations**.
- $B^0_{(s)} \to K^0_S hh'$ transitions with $h(') = \pi^\pm, K^\pm$ are part of them.
- **As a high precision science, Flavour Physics always requires the best Branching Fraction measurements**[i].

B decay mode	B^0_d	B^0_s
$K^0_S\pi^+\pi^-$	favoured	suppressed
$K^0_S K^\pm\pi^\mp$	suppressed	favoured
$K^0_S K^+K^-$	favoured	suppressed

[i] **BF($X \to y$) = probability of transition from a mother particle X to child's y.**

Goals

- Measurement of the **6 distinct $B^0_{d(s)} \to K^0_S hh'$ BF** with $h(') = \pi^\pm, K^\pm$ out of **4 experimental spectra**[ii]:
  - **search** for $B^0_s \to K^0_S K^+ K^-$,
  - **improve** the measurements of the other modes.
- **Main formula** $\Rightarrow$ **ratio of BF** relative to $B^0_d \to K^0_S \pi^+\pi^-$:

$$\frac{BF(B^0_{(s)} \to K^0_S hh')}{BF(B^0 \to K^0_S \pi^+\pi^-)} = \frac{\bar{\varepsilon}_{B^0 \to K^0_S \pi^+\pi^-}}{\bar{\varepsilon}_{B^0_{(s)} \to K^0_S hh'}} \frac{N_{B^0_{(s)} \to K^0_S hh'}}{N_{B^0 \to K^0_S \pi^+\pi^-}} \frac{f_d}{f_{d(s)}}$$

  with a ratio of average efficiencies from simulated data, a ratio of yields from an invariant-mass fit on measured data and a ratio of hadronisation fractions.
- **Starting point towards amplitude analyses** of $B^0_{(s)} \to K^0_S hh'$ to measure *CP* violation.

[ii] $\pi^+\pi^-$; K^+K^-, $K^+\pi^-$ and π^+K^-.

LHCb

- LHC : *pp* circular collider of 27 km circumference at the French-Swiss border.
- LHCb : the LHC detector which is focused on **Flavour Physics**.
- About 1400 collaborators involved in the LHCb collaboration.
- *pp* collisions recorded from 2011 to 2012 (Run1) and from 2015 to 2018 (Run2).
- **Amount of data** recorded : $9\,\mathrm{fb}^{-1}$.

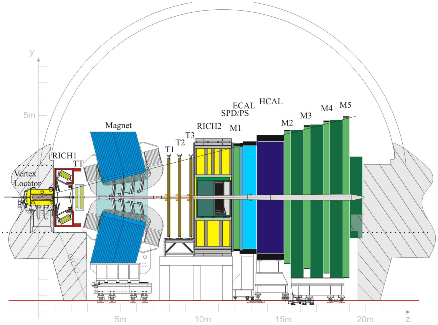

Scheme of the LHCb detector.

Previous publication [JHEP 11 (2017) 027]

- Used **Run1** 3 fb^{-1} data (against Run1+Run2 in the new analysis).
- All the modes were observed but $B^0_s \to K^0_S K^+ K^-$.
- Five BFs were measured relative to $B^0 \to K^0_s \pi^+\pi^-$ $\Rightarrow$ compatible with previous LHCb results [JHEP 10 (2013) 143].
- $\frac{BF(B^0_s \to K^0_S K^+ K^-)}{BF(B^0 \to K^0_S \pi^+\pi^-)} \in [0.008 - 0.051]@90\%\mathrm{CL}.$
- **Better particle identification** selection shall be helpful.

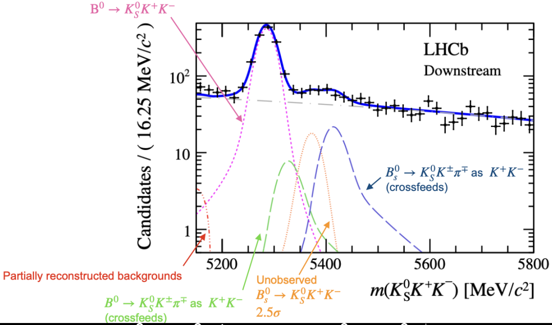

Selection

- **Not all the collisions** recorded by LHCb **contains the decays of interest** $\to$ selection needed.
- **Several stages** of selection applied to isolate $B^0_{d,(s)} \to K^0_S hh'$.
- **Two MVA's**, based on XGBoost [1], to fight the most toxic backgrounds :
  - the combinatorial backgrounds (random combination of tracks),
  - the Crossfeed backgrounds (misidentification of h or h').
- **2D optimisations** of the two MVA outputs for both the favoured and the unfavoured mode in each spectra.

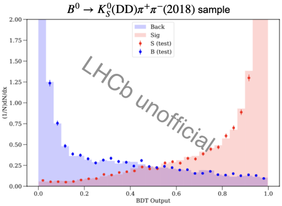

Distribution of the PID MVA (against Crossfeed) output variable $\to$ **no over-training** and **good signal-crossfeed separation**.

Yield extraction

- **Yields** are extracted for each year using **simultaneous fits** of the available samples dataset.
- **Representation of the different components** in the fit and the main regions where they contribute: signal (B^0 or B^0_s), combinatorial background, crossfeeds, partially reconstructed events, Λ_b crossfeeds.

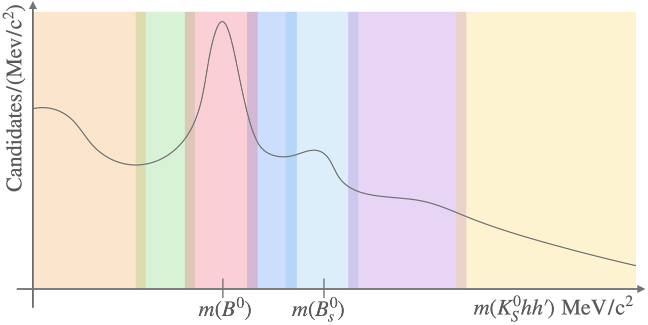

Fit model and fit results

Component	Description
B^0 peak (Signal)	Double Crystal Ball
B^0_s peak (Signal)	Double Crystal Ball
Combinatorial	Linear
Crossfeeds (2 components)	Double Crystal Ball
Partially reconstructed backgrounds (2 components)	ARGUS×Gaussian
Λ_b crossfeeds	KEYS

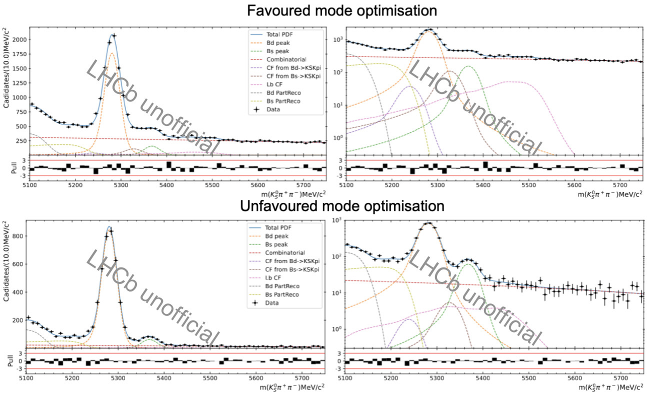

Illustration: mass fit results for a given $K^0_S\pi^+\pi^-$ 2018 spectrum.

Efficiency determination

- **MC events generated flat in the phase space** (sqDP) of the decay.
- **Efficiency maps** corresponding to **the whole selection** are built in the sqDP.
- **Various detector effects corrections included**.
- Determination of the **average efficiencies** by weighting efficiency maps w.r.t. the **phase space** (sWeights).
- I developed a **method that makes the best use of the available statistic** for all the samples[iii].

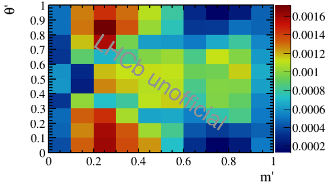

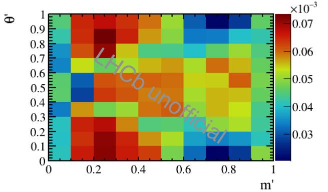

Efficiency map (top) and statistical uncertainty map (bottom) for a given $B^0 \to K^0_S\pi^+\pi^-$ 2018 sample .

[iii] To tackle observed fluctuations in the phase space of the low statistic years.

Systematics status

Several systematic uncertainties considered, evaluation in progress :

- **mass fit: varying models** ✓
- **mass fit: varying fixed parameters** ✓
- **average efficiencies: MC statistics** ✓
- **average efficiencies: method** ✓
- **data / MC corrections : various sources** ✓
- **binning scheme on the sqDP** by varying the number of bins ✓

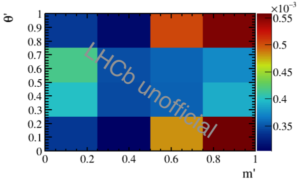

Illustration: systematics attached to the correction linked to the tracking for a $B^0 \to K^0_S\pi^+\pi^-$ 2018 sample.

Relative branching fractions measurements

- The **relative branching fractions have been extracted using results coming from the optimisation that correspond to the mode of interest**.
- Average values among years have been extracted by weighting each year w.r.t. the corresponding measured yield of $B^0 \to K^0_S\pi^+\pi^-$.
- Example of **results** (only statistic uncertainty displayed):
  $$\frac{\mathcal{B}(B^0_s \to K^0_S K^\pm\pi^\mp)}{\mathcal{B}(B^0 \to K^0_S\pi^+\pi^-)} = 1.81 \pm 0.02\,(\text{stat.}).$$
- **Previous analysis** :
  $$\frac{\mathcal{B}(B^0_s \to K^0_S K^\pm\pi^\mp)}{\mathcal{B}(B^0 \to K^0_S\pi^+\pi^-)} = 1.70 \pm 0.07\,(\text{stat.}) \pm 0.11\,(\text{syst.}) \pm 0.10\,(\mathrm{f_s/f_d}).$$
- For $B^0_s \to K^0_S K^\pm\pi^\mp$ new result is **closed to consistency** by only considering statistical uncertainty $\Rightarrow$ **expected consistent with improved precision**.

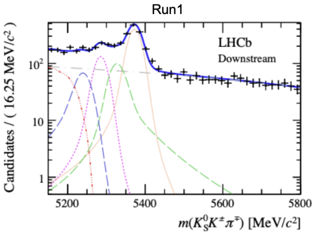

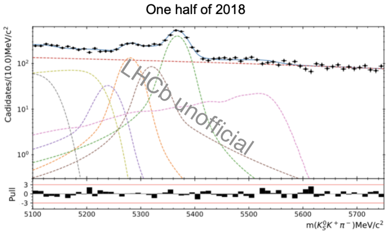

$B^0_s \to K^0_S\pi^+\pi^-$ amplitude analysis to come

- Branching fraction analysis = **starting point toward amplitude analyses**.
- I will work on **a time integrated amplitude analysis of $B^0_s \to K^0_S\pi^+\pi^-$**.
- $B^0_s \to K^0_S\pi^+\pi^-$ process through **several intermediate contributions/resonnances**.
- **Dalitz plan formalism reveal the intermediate contributions**.
- **Amplitude analysis** = fit with a model that takes into account the relevant contributions.
- **Goal : reveals direct *CP* asymmetries in $B^0_s \to K^0_S\pi^+\pi^-$**.

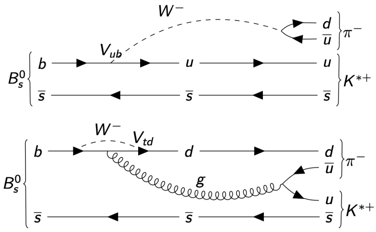

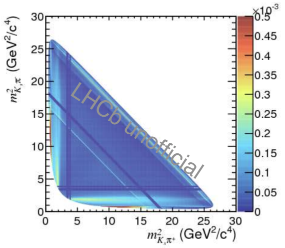

Feynman diagrams with K^{*+} resonance and preliminary Dalitz plane distribution.

$B^0_s \to K^0_S\pi^+\pi^-$ considered amplitudes and software

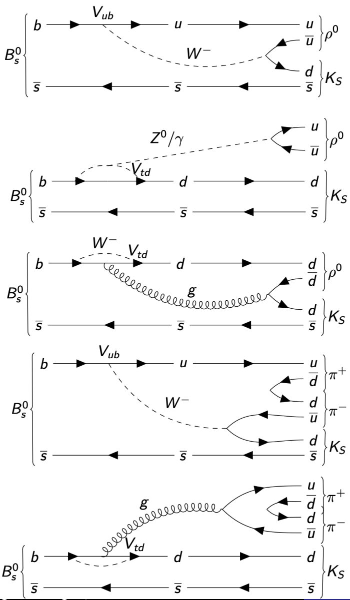

- Draw of **Feynman diagrams** to determine the **possible amplitudes**.
- Evaluating their relevance in data.
- **Amplitudes to consider**: $B^0_s \to \rho^0 K^0_S$, $B^0_s \to K^{*+}(892)\pi^-$, $B^0_s \to K^0_S\pi^+\pi^-$ (NR), $B^0_s \to K^{*+}(1430)\pi^-$.
- Software : **CRAFT** = a tool developed by a former Clermont PhD student for Dalitz amplitude analysis.
- I will try to **educate a reasonable model** with CRAFT.

Motivation and topology

- *CP* **violation study doesn't saturate the Flavour Physics** landscape.
- **BSM models** [2, 3] often **provide** $b \to \tau$ **enhancements/modifications w.r.t. the SM**.
- $b \to s\tau\tau$ ($m_\tau \sim 20 m_\mu$) is **a must do to** sort out the BSM models.
- **Problem: measuring the** ν**'s**.
- Study of the rare heavy-flavoured decay $B^0 \to K^*\tau^+\tau^-$[4]. **SM prediction**: BR=$\mathcal{O}(10^{-7})$ $\Rightarrow$ not observed yet (present limit: $\mathcal{O}(10^{-3} - 10^{-4})$ [5]).
- Work focused on the **3-prongs** τ **decays** ($\tau \to \pi\pi\pi\nu$) for which the **decay vertex can be reconstructed in order to solve fully the kinematics**.
- **10 particles** in the final state ($K, 7\pi, \nu, \bar{\nu}$), **3 decay vertices** and **2 undetected neutrinos**.

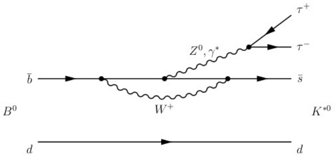

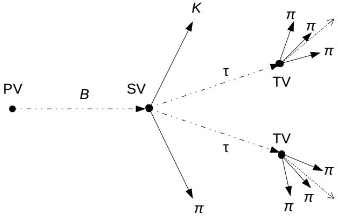

EW penguin quark-level transition and $B^0 \to K^{*0}\tau\tau$ with $\tau \to \pi\pi\pi\nu$ decay topology.

FCC-ee

- The **Future Circular Collider** is a collider project at CERN as successor of HL-LHC.
- Circumference: about 91 km.
- **FCC**-*ee* **is the first phase of the project** with *ee* collision.
- 4 interaction points in the FCC-*ee* baseline and **4 data taking years at the** Z **pole** $\to N_Z = 6 \times 10^{12}$.
- FCC-*ee* : combined **clear experimental environment** (like B-factories with more Z bosons) and **boosted** b **hadrons** (like *LHC*).
- FCC-*ee* = **right place** to reconstruct the ν's and to study $B^0 \to K^{*0}\tau\tau$.

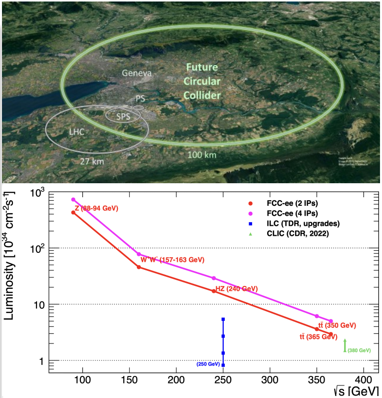

FCC plan and FCC-*ee* comparison in term of luminosity comparing to other projects.

Goal: explore the feasibility of the search for $B^0 \to K^*\tau^+\tau^-$ **at FCC**-*ee* **and give the corresponding vertex detector requirements.**

Reconstruction method

- To fully reconstruct the kinematics of the decay $\rightarrow$ **neutrinos momenta must be resolved**.
- **Enough constraints are available** in order to determine the missing coordinates.
- **Energy momentum conservation at τ decay vertex** $\Rightarrow$ gives the **neutrino momentum** at the cost of a **quadratic ambiguity**:

$$\begin{cases} p^{\perp}_{\nu_\tau} = -p^{\perp}_{\pi_t} \\ p^{\parallel}_{\nu_\tau} = \dfrac{((m^2_\tau - m^2_{\pi_t}) - 2p^{\perp,2}_{\pi_t})}{2(p^{\perp,2}_{\pi_t} + m^2_{\pi_t})}.p^{\parallel}_{\pi_t} \pm \dfrac{\sqrt{(m^2_\tau - m^2_{\pi_t})^2 - 4m^2_\tau p^{\perp,2}_{\pi_t}}}{2(p^{\perp,2}_{\pi_t} + m^2_{\pi_t})}.E_{\pi_t} \end{cases}$$

- A **selection rule** has to be build in order **to solve the ambiguities**.
- Practically **energy-momentum conservation at the B decay vertex** gives a **condition between τ's and K^***:

$$p_{\tau^+_-} = -\frac{\vec{p}^{\perp}_{K*}.\vec{e}_{\tau^+_-}}{1-(\vec{e}_{\tau^+_-}.\vec{e}_B)^2} - p_{\tau^-_+}.\frac{\vec{e}_{\tau^+_-}.\vec{e}_{\tau^-_+} - (\vec{e}_{\tau^+_-}.\vec{e}_B)(\vec{e}_{\tau^-_+}.\vec{e}_B)}{1-(\vec{e}_{\tau^+_-}.\vec{e}_B)^2}$$

- **Method validated at MC truth level**.

Backgrounds

- **In addition** of the signal, the **main backgrounds** (similar final state to the signal) have been **considered** (simulations).
- Even with arbitrarily **good calorimeter performances, backgrounds are overwhelming**.
- A **selection is needed**.

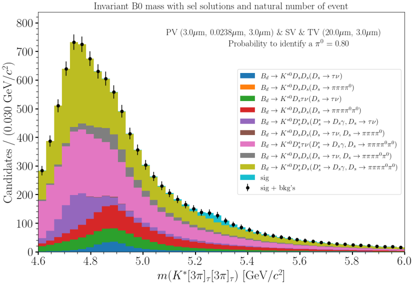

Decay	BF (SM/meas.)	Intermediate decay	BF_had	Additional missing particles
Backgrounds $b \to c\bar{c}s$:				
$B^0 \to K^{*0} D_s D_s$	5.47×10^{-5}	$D_s \to \tau\nu$	1.14×10^{-10}	2ν
		$D_s \to \tau\nu, \pi\pi\pi\pi^0$	1.28×10^{-10}	ν , π^0
		$D_s \to \pi\pi\pi\pi^0$	1.45×10^{-10}	$2\pi^0$
		$D_s \to \tau\nu, \pi\pi\pi\pi^0\pi^0$	1.08×10^{-9}	ν , $2\pi^0$
		$D_s \to \pi\pi\pi 2\pi^0$	1.02×10^{-8}	$4\pi^0$
$B^0 \to K^{*0} D_s D_s^*$	1.73×10^{-4}	$D_s \to \tau\nu$	3.60×10^{-10}	2ν, γ/π^0
		$D_s \to \pi\pi\pi\pi^0\pi^0$	3.22×10^{-8}	$4\pi^0$, γ/π^0
Backgrounds $b \to c\tau\nu$:				
$B^0 \to K^{*0} D_s \tau\nu$	9.17×10^{-6}	$D_s \to \tau\nu$	3.59×10^{-10}	2ν
$B^0 \to K^{*0} D_s^* \tau\nu$	2.03×10^{-5}	$D_s \to \pi\pi\pi\pi^0\pi^0$	7.51×10^{-9}	ν, γ, $2\pi^0$

Selection

- Several **discriminative variables** found such as intermediate candidates momentum or flight distances.
- **XGBoost [1] selection** fed with the available variables.
- **Better definition of the signal peak.**

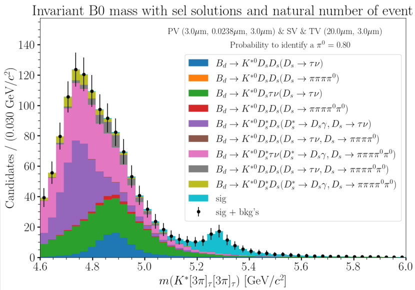

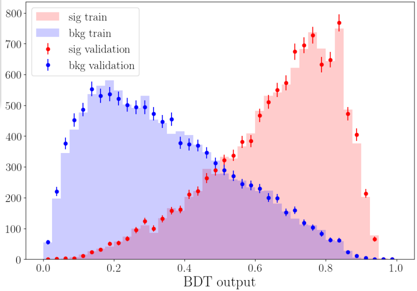

Precision on the BF measurement

- **Precision** on the BF measurement determined for **several vertexing performance emulations**.
- Precision from a **fit to the reconstructed B^0 invariant mass**.
- Signal : double CB + core gaussian model.
- Background : two decreasing exponential's.
- **Extraction of the signal yields N and uncertainties σ_N.**
- **Precision on the BF measurement** given by σ_N/N.

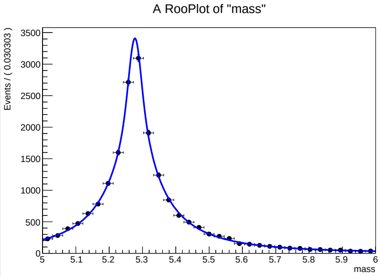

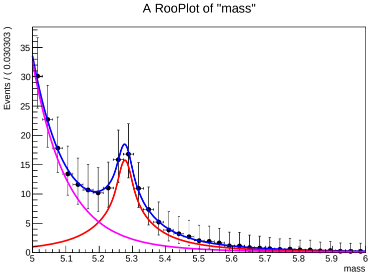

Results

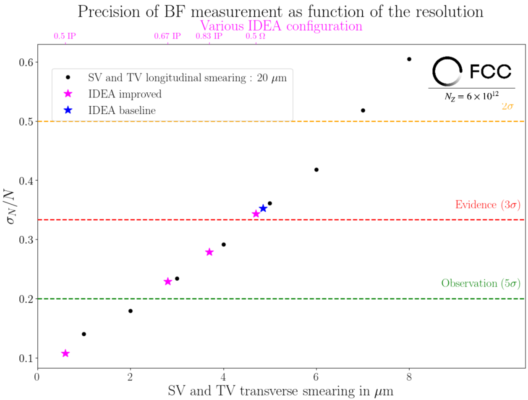

- **Hint of the signal with the state-of-the-art vertex detector** (IDEA[6]).
- **Improvement of the Impact Parameters measurement can improve the picture**.
- On the other hand, considering **leptonic τ decays** improve the statistic $\to$ requires other methods for the reconstruction.

End

Thanks for your attention !

Trigger

List of trigger requirements used for each year. A logical OR is implied between each line and a logical AND is implied between the columns. Mid 2012 : major changes have been made to the HLT2 topological lines → split in two part 2012a and 2012b in the following.

Year	Trigger requirements	HLT1 trigger requirements	HLT2 trigger requirements
2011	B_L0HadronDecision_TOS B_L0DiMuonDecision_TIS B_L0MuonDecision_TIS B_L0ElectronDecision_TIS B_L0PhotonDecision_TIS B_L0HadronDecision_TIS	B_Hlt1TrackAllL0Decision_TOS	B_Hlt2Topo2BodyBBDTDecision_TOS B_Hlt2Topo3BodyBBDTDecision_TOS B_Hlt2Topo4BodyBBDTDecision_TOS B_Hlt2Topo2BodySimpleDecision_TOS B_Hlt2Topo3BodySimpleDecision_TOS B_Hlt2Topo4BodySimpleDecision_TOS
2012	(same as 2011)	(same as 2011)	B_Hlt2Topo2BodyBBDTDecision_TOS B_Hlt2Topo3BodyBBDTDecision_TOS B_Hlt2Topo4BodyBBDTDecision_TOS
2015	B_L0HadronDecision_TOS B_L0DiMuonDecision_TIS B_L0MuonDecision_TIS B_L0ElectronDecision_TIS B_L0PhotonDecision_TIS B_L0HadronDecision_TIS B_L0MuonEWDecision_TIS B_L0MuonNoSPDDecision_TIS B_L0JetElDecision_TIS B_L0JetPhDecision_TIS	B_Hlt1TrackMVADecision_TOS B_Hlt1TwoTrackMVADecision_TOS	B_Hlt2Topo2BodyDecision_TOS B_Hlt2Topo3BodyDecision_TOS B_Hlt2Topo4BodyDecision_TOS
2016, **2017**, **2018**	B_L0HadronDecision_TOS B_L0DiMuonDecision_TIS B_L0MuonDecision_TIS B_L0ElectronDecision_TIS B_L0PhotonDecision_TIS B_L0HadronDecision_TIS B_L0MuonEWDecision_TIS B_L0JetElDecision_TIS B_L0JetPhDecision_TIS	(same as 2015)	(same as 2015)

Preselection and vetoes

Preselection cuts.

Preselection cut	Description
B_STRIP_VTXISOCHI2ONETRACK > 4	B vertex isolation variable
KS_ENDVERTEX_Z $-$ B_ENDVERTEX_Z > 30	K^0_S vertex separation w.r.t. the B vertex
h{1,2}_isMuon == 0	Reject $h^{(\prime)}$ candidates compatible with the muon hypothesis
$3000 \leq p(h^{(\prime)}) \leq 100000$	Fiducial cut
$\min\chi^2_{\rm IP}(h^{(\prime)}) > 4$	Minimum IP χ^2 of the charged daughters with respect to the related PV
$p_T(h^{(\prime)})>250$ MeV	Minimum transverse momentum of the charged daughters.

Charm vetoes applied.

$$D^{\pm} \to \pi^{\pm} K^0_S,\ D^{\pm} \to K^{\pm} K^0_S$$
$$D^{\pm}_s \to \pi^{\pm} K^0_S,\ D^{\pm}_s \to K^{\pm} K^0_S$$
$$D^0 \to \pi^+\pi^-,\ D^0 \to K^+K^-,\ D^0 \to K^{\pm}\pi^{\mp}$$
$$\Lambda^+_c \to p K^0_S$$
$$J/\Psi \to \pi^+\pi^-,\ J/\Psi \to K^+K^-$$
$$\chi_{c,0} \to \pi^+\pi^-,\ \chi_{c,0} \to K^+K^-$$

MVA of topological variables

- Used to reduce the amount of **combinatorial background**.
- **Discriminating variables that are uncorrelated to the B mass and to the Dalitz-plot position**.
- **Trained on $B_d^0 \to K_S^0\pi^+\pi^-$ samples** with signal from MC and backgrounds in upper sideband of the data samples.

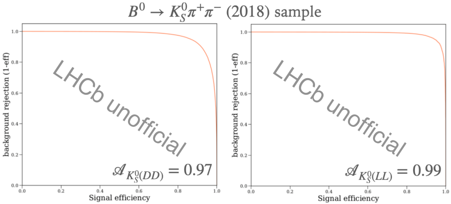

ROC curves for the topological MVA, the area under the curves is displayed and shows a **good background-signal separation**.

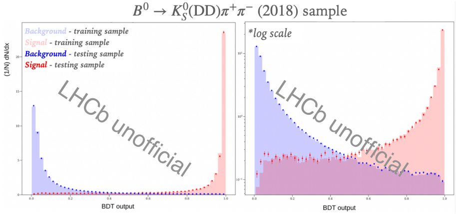

Distribution of the topological MVA output variable, similar performances are showns on training and testing samples $\to$ **satisfactory training**.

MVA of PID variables

- Used to reduce the amount of **crossfeeds** (e.g. backgrounds arising from h or h' miss identification).
- Use of the **ProbNN variables**, **corrected via PIDCorr method** to tackle known data-MC discrepancies, for kaons, pions and protons.
- **Trained on MC samples** for signal and crossfeeds.

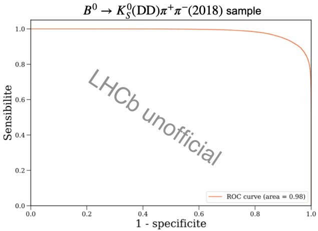

ROC curve for the PID MVA, the area under the curves is displayed and shows a **good crossfeed-signal separation**.

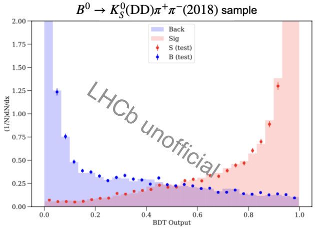

Distribution of the PID MVA output variable, similar performances are shown on training and testing samples $\rightarrow$ **no over-training**.

2D optimisation:FoM

- Signal significance for the observed modes:

$$\mathrm{FoM} = \frac{\mathrm{S}}{\sqrt{\mathrm{S}+\mathrm{B}}},$$

where S and B are respectively the number of signal and background events.

- Punzi FoM for the unobserved mode:

$$\mathrm{FoM}_{\mathrm{Punzi}} = \frac{\epsilon_{\mathrm{sig}}}{\frac{\mathrm{a}}{2}+\sqrt{\mathrm{B}}},$$

where ϵ_{sig} is the signal efficiency, a is a "small number" of standard deviations at which the null hypothesis would be rejected (just for the purposes of this optimisation) set to 5 in the analysis.

Mass fit: B^0 and B^0_s signal

- Definition: events that are coming from the decays of interest.
- Model description : each signal peak (B^0 and B^0_s) is modelled with a double Crystal Ball (sum of left and right Crystal Ball functions) using the RooFit RooCBShape class. One Crystal Ball (CB) lineshape is given by:

$$PDF_{CB,i}(x) = N \begin{cases} \exp(-\frac{t^2}{2}) & \text{if } t > -\alpha_i \\ \frac{1}{(\frac{n_i-\alpha_i^2}{|\alpha_i|} - t)^{n_i}} \left(\frac{n_i}{|\alpha_i|}\right)^{n_i} \exp(-\frac{\alpha_i^2}{2}) & \text{if } t \leq -\alpha_i \end{cases}, t = \frac{x-\mu}{\sigma}.$$

- Fit to MC samples: 18 parameters are fitted per year (means μ, widths $\sigma(B^0)(\pi\pi)(DD)$ and $\sigma_r(XX)$ w.r.t. the $(B^0)(\pi\pi)(DD)$ reference for other samples, left-handed tail parameters, right handed tail parameters relative to the left ones, fraction of right handed CB).
- Fit to data: μ_{B^0} ($\mu_{B^0_s}$ is constrained by the known $\mu_{B^0_s} - \mu_{B^0} = 87.26\,\text{MeV/c}^2$), width $\sigma(B^0)(\pi\pi)(DD)$, yields ($B^0_s \to K^0_S KK$ is blinded).

Mass fit: crossfeeds backgrounds

- Definition: events where one of the final state hadrons has been misidentified to form the final state of another studied decay, for example $B^0 \to K_S^0\pi\pi$ found in the $K_S^0\pi K$ spectrum. These contributions overlap with the signal tails and can affect the extracted signal yields. Only single misidentified decays are taken into account, doubly misidentified crossfeeds have been studied and found to be negligible compared to single misidentified decays $\to$ two sources of crossfeeds per mode.
- Model description : double Crystal Ball (like signal).
- Fit to MC samples: each crossfeed mode is taken to have the same shape across the years (fit of the double CB shape).
- Fit to data: due to low statistic the fit with the unfavoured optimisation not converge $\to$ for them shape is taken from the favoured optimisation fit, the misidentification efficiencies + the measurement yield of the source of the crossfeed allow to estimate the yields of the crossfeed contributions.

Mass fit: partially reconstructed backgrounds

- Definition: events accounting for decays such as $X \to K^0_S hh' Y$, where Y is not being reconstructed (too soft or out the LHCb acceptance). Four canonical modes are considered ($B^+ \to D^0(K^0_S\pi^+\pi^-)\pi^+$, $B^0 \to K^{*0}(K^0_S\pi^0)\rho^0(\pi^+\pi^-)$, $B^0 \to \eta'(\rho^0\gamma)K^0_S$, $B^0 \to K^0_S\pi^+\pi^-\gamma$).
- Model description : ARGUS function convoluted with a Gaussian distribution (μ, σ) via RooArgusBG and RooGaussian.

$$PDF_{ARGUS}(x) = Nm\left[1 - \left(\frac{m}{m_t}\right)^2\right]^p \exp\left[c\left(1 - \left(\frac{m}{m_t}\right)^2\right)\right],$$

  with N the normalisation factor, p the curvature, c the slope and m_t the threshold.
- Fit to MC samples: shapes from fits to simulated partially reconstructed backgrounds in the $K^0_S\pi\pi$ spectra, shared with the other spectra.
- Fit to data: shifted threshold w.r.t. $m_{B^0_s} - m_{B^0}$ to model B^0_s partially reconstructed, only partially reconstructed charmless decays modelled (systematic to compensate others), yields of the partially reconstructed charmless decays are left floating, yields of the partially reconstructed radiative decays (resonant and non-resonant) are fixed to the estimate values thanks to their known branching fractions.

Mass fit: Λ_b^0 crossfeeds backgrounds

- Definition: $\Lambda_b^0 \to K_S^0 ph$ where p is misidentified as π or k, lie after the second signal peak.
- Model description : strongly shaped by the PID BDT-selections $\to$ no general lineshape $\Rightarrow$ modelled with KEYS (shape from Kernel Estimations) via RooKeysPdf class.
- Fit to MC samples: each sample (year/K_S^0reconstruction/final state) is fitted individually.
- Fit to data: yields are left floating.

Mass fit: combinatorial backgrounds

- Definition: dominant source of background. originates from random combinations of tracks and of other sources of background not explicitly accounted for.
- Model description : linear function (first order Chebychev polynomial), implemented using the RooChebychev class.
- Fit to data: slope is left free to vary. The $K^+\pi^-$ and π^+K^- spectra are considered to have the same combinatorial slope. Slope expected to be negative but positive slope might happen $\rightarrow$ slope fixed to 0.

Fit requirements

Requirement	Description
covQual = 3	Fully accurate covariance matrix (after MIGRAD)
$edm < 0.01$	Expeted distance to minimum
fitStatus = 0	Overall variable that characterises the goodness of the fit

Fit results on the favoured mode optimisation

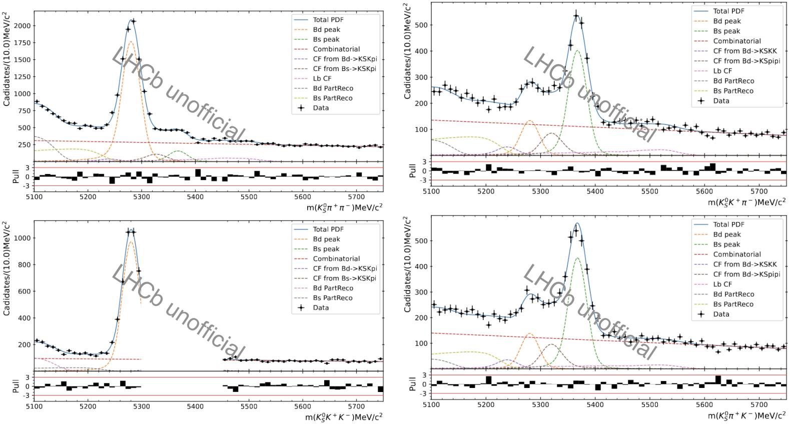

Illustration of the mass fit results for DD K_S^0 reconstruction, 2018 for the favoured mode optimisation.

Method

- Because of the upcoming amplitude analyses of $B \to K^0_S hh'$, the efficiencies are determined across the phase space of the decay.
- MC generated flat in the square Dalitz plane in order to enhanced the relevant physics region.
- The total efficiency to determine is

$$\epsilon^{\text{tot}} = \epsilon^{\text{geom}} \times \epsilon^{\text{sel|geom}} \times \epsilon^{\text{PID|Sel\&geom}}$$

  with:

  - ϵ^{geom} is the geometrical and generator level cut efficiency determined using MC samples.
  - $\epsilon^{\text{sel|geom}}$ is the selection efficiency which consists of the trigger, stripping and offline selection (except for the PID MVA selector), also determined from the MC sample with corrections of discrepancies between the data and MC in the tracking and trigger efficiencies.
  - $\epsilon^{\text{PID|Sel\&geom}}$ is the efficiency of the particle identification requirements, determined by using the output of the MVA PID selector on MC samples.

- The samples generated to determine the efficiencies are taken into account the two different polarities of the LHCb magnet, an efficiency is determined for each magnet polarity.

Efficiency determination

- ϵ^{geom} is determined following a given a set of generator level cut, no K_S^0 reconstruction type separation is needed because this efficiency only depends on the detector geometry and the B^0 kinematics.
- The tracking efficiency corrections are made according the usual correction tables provided by the tracking group (p, η) applying to the MC samples that passed the selection (but the PID MVA).
- The trigger L0HadronTOS efficiency corrections are made following the data driven method developed on RunII which have been generalized to RunI+RunII.
- As an illustration the corresponding $B^0 \to K_S^0 \pi^+ \pi^-$ maps for 2018, DD, MD are given on the right.

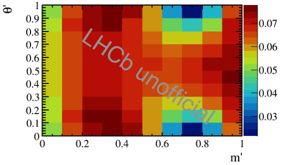

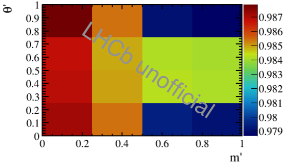

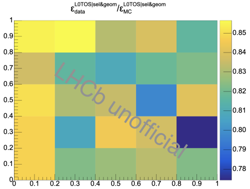

Corrected efficiency determination

- The total efficiency is build by applying the whole selection to the MC sample.
- The efficiency to consider has to be corrected from the tracking and trigger effects using the aforementioned correction maps.
- The corrected efficiency is given by:

$$\epsilon_{corrected} = (\epsilon_{TOS} \times C_{TOS} + \epsilon_{!TOS}) \times C_{tracking}$$

  where:

  - $\epsilon_{(!)TOS}$ is the total efficiency attached to the (not) TOS events,
  - C_{TOS} is the L0Hadron TOS correction,
  - $C_{tracking}$ is the tracking correction.
- One corrected efficiency map is build for each of the previous sample and for each type of selection optimisation.

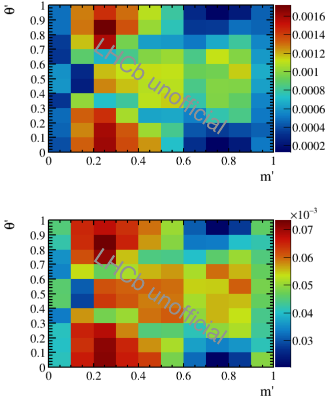

Corrected efficiency map (top) and statistical uncertainty map (bottom) builds for $B^0 \to K^0_S\pi^+\pi^-$, 2018, DD, MD with the favoured mode optimisation.

Average efficiency definition

- **Average efficiencies** obtained by **weighting the MC flat sqDP maps** by the actual position of the data points (invariant mass sFit's).
- In order to make the **best use of the statistics** 2016, 2017 and 2018 data samples **sWeights** are fed into each and every efficiency year determination:

$$\bar{\varepsilon}_k = \sum_{k'} \bar{\varepsilon}_{k,k'} / \sum_{k'} 1$$

with:

$$\bar{\varepsilon}_{k,k'} = \frac{\sum_j sW_{k',j} \varepsilon_{k',j}^{-1} \varepsilon_{k,j}}{\sum_j sW_{k',j} \varepsilon_{k',j}^{-1}}$$

where k and k' denote respectively the index of the period for which the average efficiency is determined and the index of the period use as reference in the computation, j denotes a sqDP bin. The efficiency ratio in red allow to compute the average efficiency of one period given the phase space of another one.

- During the development of the method $\rightarrow$ observation of fluctuations in the phase space of low statistic periods $\Rightarrow$ accounted by the method.
- Statistical **uncertainties** attached to this formula are **split in three contributions** (the size of the MC sample of the computed year, the size of the MC sample of the reference year and the spread of the average efficiencies over the reference years)

Average efficiency: uncertainty formula

- The uncertainty per period is written as:

$$\sigma^2_{\bar{\varepsilon}_k} = \sigma^2_{\bar{\varepsilon}_\mathbf{1}} + \sigma^2_{\bar{\varepsilon}_\mathbf{2}} + \sigma^2_{\bar{\varepsilon}_\mathbf{3}},$$

- $\sigma^2_{\bar{\varepsilon}_\mathbf{1}}$ is the uncertainty attached to the current period, the uncertainty maps used is the same $\rightarrow$ arithmetic mean over reference year is taken:

$$\sigma_{\bar{\varepsilon}_\mathbf{1}} = \frac{\sum_{k'} \sqrt{\sum_j \left(\frac{\partial \bar{\varepsilon}_{k,k'}}{\partial \varepsilon_{k,j}} \sigma_{\varepsilon_{k,j}} \right)^2}}{\sum_{k'} 1} = \frac{\sum_{k'} \sqrt{\frac{\sum_j (sW_{k',j} \varepsilon^{-1}_{k',j} \sigma_{\varepsilon_{k,j}})^2}{(\sum_{j'} sW_{k',j'} \varepsilon^{-1}_{k',j'})^2}}}{\sum_{k'} 1}$$

- $\sigma^2_{\bar{\varepsilon}_\mathbf{3}}$ is an uncertainty attached to the distribution of the average efficiency, it can be seen as an uncertainty on the sWeights attached on each period:

$$\sigma_{\bar{\varepsilon}_\mathbf{3}} = RMS(\bar{\varepsilon}_k - \bar{\varepsilon}_{k,k'})$$

Average efficiency: uncertainty formula

- $\sigma^2_{\bar{\bar{\varepsilon}}_{\mathbf{2}}}$ is the uncertainty attached to the reference period, the uncertainty maps change for each reference period → a weighted average is taken:

$$\frac{1}{\sigma^2_{\bar{\bar{\varepsilon}}_{\mathbf{2}}}} = \sum_{k'} \frac{1}{\sigma^2_{\bar{\bar{\varepsilon}}_{\mathbf{2}k'}}},$$

where:

$$\sigma^2_{\bar{\bar{\varepsilon}}_{\mathbf{2}k'}} = \sum_j \left(\frac{\partial \bar{\varepsilon}_{k,k'}}{\partial \varepsilon_{k',j}} \sigma_{\varepsilon_{k',j}} \right)^2 = \frac{1}{(\sum_{j'} sW_{k',j'} \varepsilon^{-1}_{k',j'})^4}$$

$$[\sum_j (sW_{k',j} \varepsilon^{-2}_{k',j} \sigma_{\varepsilon_{k',j}})^2 (\sum_{j'} sW_{k',j'} \varepsilon^{-1}_{k',j'} \varepsilon_{k,j'})^2 +$$

$$\sum_j (sW_{k',j} \varepsilon^{-2}_{k',j} \varepsilon_{k,j} \sigma_{\varepsilon_{k',j}})^2 (\sum_{j'} sW_{k',j'} \varepsilon^{-1}_{k',j'})^2 -$$

$$\sum_j 2(sW^2_{k',j} \varepsilon^{-4}_{k',j} \varepsilon_{k,j} \sigma^2_{\varepsilon_{k',j}})(\sum_{j'} sW_{k',j'} \varepsilon^{-1}_{k',j'} \varepsilon_{k,j'})(\sum_{j'} sW_{k',j'} \varepsilon^{-1}_{k',j'})]$$

Previous measurements

- $\frac{\mathcal{B}(B^0 \to K^0_S K^\pm \pi^\mp)}{\mathcal{B}(B^0 \to K^0_S \pi^+ \pi^-)} = 0.123 \pm 0.009\,(\text{stat.}) \pm 0.015\,(\text{syst.})$
- $\frac{\mathcal{B}(B^0 \to K^0_S K^+ K^-)}{\mathcal{B}(B^0 \to K^0_S \pi^+ \pi^-)} = 0.549 \pm 0.018\,(\text{stat.}) \pm 0.033\,(\text{syst.})$
- $\frac{\mathcal{B}(B^0_s \to K^0_S \pi^+ \pi^-)}{\mathcal{B}(B^0 \to K^0_S \pi^+ \pi^-)} = 0.191 \pm 0.027\,(\text{stat.}) \pm 0.031\,(\text{syst.}) \pm 0.011(f_s/f_d)$
- $\frac{\mathcal{B}(B^0_s \to K^0_S K^\pm \pi^\mp)}{\mathcal{B}(B^0 \to K^0_S \pi^+ \pi^-)} = 1.70 \pm 0.07\,(\text{stat.}) \pm 0.11\,(\text{syst.}) \pm 0.10(f_s/f_d)$

FCC : neutrinos reconstruction method

To fully reconstruct the kinematics of the decay (B invariant-mass observable for instance) we need :

- Momentum of all final particles including not detected neutrinos.
- The decay lengths (6 constraints) together with the tau mass (2 constraints) can be used to determine the missing coordinates (6 degrees of freedom).
- We use energy-momentum conservation at tertiary (or τ decay) vertex with respect to τ direction [iv].

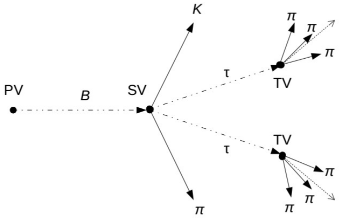

Figure: The dotted lines represent the non-reconstructed particles. The plain lines are the particles that can be reconstructed in the detector.

$$\begin{cases} p^{\perp}_{\nu_\tau} = -p^{\perp}_{\pi_t} \\ p^{\parallel}_{\nu_\tau} = \dfrac{((m^2_\tau - m^2_{\pi_t}) - 2p^{\perp,2}_{\pi_t})}{2(p^{\perp,2}_{\pi_t} + m^2_{\pi_t})}.p^{\parallel}_{\pi_t} \pm \dfrac{\sqrt{(m^2_\tau - m^2_{\pi_t})^2 - 4m^2_\tau p^{\perp,2}_{\pi_t}}}{2(p^{\perp,2}_{\pi_t} + m^2_{\pi_t})}.E_{\pi_t} \end{cases}$$

[iv] Another way to do this computation is given by [7].

FCC : selection rule

There is a quadratic ambiguity on each neutrino momentum !

$\rightarrow$ The ambiguities propagate to τ and B reconstructions

$\rightarrow$ 4 possibilities by taking all +/- combination for the two neutrinos

$\Rightarrow$ A selection rule is needed to choose the right possibility

$\longrightarrow$ From the energy-momentum conservation at the B decay vertex, we have a condition between the 2 taus and the K^* with respect to the B direction:

$$p_{\tau^{+}_{-}} = -\frac{\vec{p}^{\perp}_{K*}.\vec{e}_{\tau^{+}_{-}}}{1-(\vec{e}_{\tau^{+}_{-}}.\vec{e}_B)^2} - p_{\tau^{-}_{+}}.\frac{\vec{e}_{\tau^{+}_{-}}.\vec{e}_{\tau^{-}_{+}} - (\vec{e}_{\tau^{+}_{-}}.\vec{e}_B)(\vec{e}_{\tau^{-}_{+}}.\vec{e}_B)}{1-(\vec{e}_{\tau^{+}_{-}}.\vec{e}_B)^2}$$

FCC : simulation

- Signal and dominant backgrounds generated with Pythia [8] and EvtGen [9].
- Reconstruction is performed with the FCC Analyses sw using Delphes [10] simulation featuring the IDEA [6] detector.
- Particles reconstruted with IDEA momentum resolution.
- To investigate vertexing detector requirements $\rightarrow$ secondary vertexing resolution working points emulated along longitudinal and transverse directions to the decaying particles w.r.t. expectations and IDEA baseline.

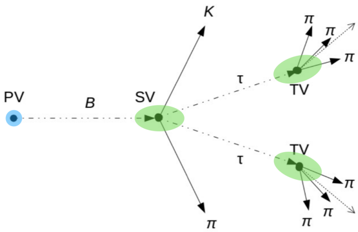

Figure: Vertexing performances emulation.

FCC : The considered backgrounds

- The relevant backgrounds are the ones with a similar final state than the signal ($K7\pi$).
- Several possible modes in $b \to c\bar{c}s$ and $b \to c\tau\nu$ transitions [v] but often not observed to date $\Rightarrow$ guesstimate of the branching fraction from phase space computation and use of analogies.
- Determination of the dominant backgrounds for the measurement by building per track efficiencies from already generated ones.

Decay	BF (SM/meas.)	Intermediate decay	BF_had	Additional missing particles
Signal: $B^0 \to K^*\tau\tau$	1.30×10^{-7}	$\tau \to \pi\pi\pi\nu$, $K^* \to K\pi$	9.57×10^{-11}	
Backgrounds $b \to c\bar{c}s$:				
$B^0 \to K^{*0}D_sD_s$	5.47×10^{-5}	$D_s \to \tau\nu$	1.14×10^{-10}	2ν
		$D_s \to \tau\nu, \pi\pi\pi\pi^0$	1.28×10^{-10}	ν , π^0
		$D_s \to \pi\pi\pi\pi^0$	1.45×10^{-10}	$2\pi^0$
		$D_s \to \tau\nu, \pi\pi\pi\pi^0\pi^0$	1.08×10^{-9}	ν , $2\pi^0$
		$D_s \to \pi\pi\pi2\pi^0$	1.02×10^{-8}	$4\pi^0$
$B^0 \to K^{*0}D_sD_s^*$	1.73×10^{-4}	$D_s \to \tau\nu$	3.60×10^{-10}	2ν, γ/π^0
		$D_s \to \pi\pi\pi\pi^0\pi^0$	3.22×10^{-8}	$4\pi^0$, γ/π^0
Backgrounds $b \to c\tau\nu$:				
$B^0 \to K^{*0}D_s\tau\nu$	9.17×10^{-6}	$D_s \to \tau\nu$	3.59×10^{-10}	2ν
$B^0 \to K^{*0}D_s^*\tau\nu$	2.03×10^{-5}	$D_s \to \pi\pi\pi\pi^0\pi^0$	7.51×10^{-9}	ν, γ, $2\pi^0$

[v] More details on backgrounds choices in appendix.

FCC : extended background table

Decay	BF (SM/meas.)	Intermediate decay	BF_had	Additional missing particles
Signal: $B^0 \to K^* \tau\tau$	1.30×10^{-7}	$\tau \to \pi\pi\pi\nu$, $K^* \to K\pi$	9.57×10^{-11}	
Backgrounds $b \to c\bar{c}s$:				
$B^0 \to K^{*0} D_s D_s$	5.47×10^{-5}	$D_s \to \tau\nu$	1.14×10^{-10}	2ν
		$D_s \to \tau\nu, \pi\pi\pi\pi^{0}$[vi]	1.28×10^{-10}	ν , π^0
		$D_s \to \pi\pi\pi\pi^{0}$[vi]	1.45×10^{-10}	$2\pi^0$
		$D_s \to \tau\nu, \pi\pi\pi\pi^0\pi^0$	1.08×10^{-9}	ν , $2\pi^0$
		$D_s \to \pi\pi\pi 2\pi^{0}$[vi]	1.02×10^{-8}	$4\pi^0$
$B^0 \to K^{*0} D_s D_s^*$	1.73×10^{-4}	$D_s \to \tau\nu$	3.60×10^{-10}	2ν, γ/π^0
		$D_s \to \tau\nu, \pi\pi\pi\pi^0$	4.06×10^{-10}	ν , π^0, γ/π^0
		$D_s \to \pi\pi\pi\pi^0$	4.57×10^{-10}	$2\pi^0$, γ/π^0
		$D_s \to \pi\pi\pi\pi^0\pi^0$	3.22×10^{-8}	$4\pi^0$, γ/π^0
$B^0 \to K^{*0} D_s^* D_s^*$	1.79×10^{-4}	$D_s \to \tau\nu$	3.73×10^{-10}	2ν, $2\gamma/\pi^0$
		$D_s \to \tau\nu, \pi\pi\pi\pi^0$	4.20×10^{-10}	ν , π^0, $2\gamma/\pi^0$
		$D_s \to \pi\pi\pi\pi^0$	4.73×10^{-10}	$2\pi^0$, $2\gamma/\pi^0$
Backgrounds $b \to c\tau\nu$:				
$B_s \to K^{*0} D\tau\nu$	7.27×10^{-5}	$D \to \pi\pi\pi\pi^0$	1.65×10^{-9}	ν, π^0
$B_s \to K^{*0} D^*\tau\nu$	2.03×10^{-4}	$D^* \to D^0\pi, D\pi^0$		
		$D \to \pi\pi\pi\pi^0$	1.12×10^{-9}	ν, $2\pi^0$
		$D^0 \to 2\pi 2\pi\pi^0$	8.98×10^{-10}	ν, $2\pi^0$, $2\pi^{\pm}$
$B^0 \to K^{*0} D_s\tau\nu$	9.17×10^{-6}	$D_s \to \tau\nu$	3.59×10^{-10}	2ν
		$D_s \to \pi\pi\pi\pi^0$	4.05×10^{-10}	ν, π^0
$B^0 \to K^{*0} D_s^*\tau\nu$	2.03×10^{-5}	$D_s \to \tau\nu$	8.07×10^{-10}	2ν, γ/π^0
		$D_s \to \pi\pi\pi\pi^0$	9.09×10^{-10}	ν, π^0, γ/π^0
		$D_s \to \pi\pi\pi\pi^0\pi^0$	7.51×10^{-9}	ν, γ, $2\pi^0$

[vi] $D_s \to 3\pi n\pi^0$ modes involves η/ω intermediate states.

FCC : Some words about guesstimation of the BF for unseen modes

- $B^0 \to K^{*0} D_s D_s$ guesstimate from recent LHCb measurement [11]:

$$BF(B^0 \to K^{*0} D_s D_s) = BF(B^+ \to K^+ D_s^+ D_s^-) \times C_{\mathrm{FF}} \times C_{\mathrm{PS}},$$

  where $B^+ \to K^+ D_s^+ D_s^-$ has the same quark content but the spectator w.r.t. $B^0 \to K^{*0} D_s D_s$,
  $C_{\mathrm{FF}} = \mathrm{FF}_{\mathrm{K}^*}/\mathrm{FF}_{\mathrm{K}} = \mathrm{BF}(\mathrm{B}^+ \to \mathrm{D}^0 \mathrm{K}^{*+})/\mathrm{BF}(\mathrm{B}^+ \to \mathrm{D}^0 \mathrm{K}^+)$ and
  $C_{\mathrm{PS}} = PS(B^+ \to K^{*+} D_s^+ D_s^-)/PS(B^+ \to K^+ D_s^+ D_s^-)$.
- $B^0 \to K^{*0} D_s^* D_s$ and $B^0 \to K^{*0} D_s^* D_s^*$ w.r.t. $B^0 \to K^{*0} D_s D_s$ from $B_s^0 \to D_s^{(*)} D_s^{(*)}$ hierarchy.
- $B^0 \to K^{*0} D_s^{(*)} \tau\nu$ from analogy via phase space computation[7]:

$$BF(B^0 \to K^{*0} D_s^{(*)} \tau\nu) = BF(B^+ \to K D_s^{(*)} \ell\nu) \times \frac{PS(B^0 \to K^{*0} D_s^{(*)} \tau\nu)}{PS(B^+ \to K D_s^{(*)} \ell\nu)}$$

  where PS denotes the Phase Space computed numerricaly (three body decay hypothesis used conservatively) and $B^+ \to K D_s^{(*)} \ell\nu$ is a reference mode with a known BF.
- $B^0 \to K^{*0} D_s \tau\nu$ and $B^0 \to K^{*0} D_s^* \tau\nu$ w.r.t $B^0 \to K^{*0} D_s^{(*)} \tau\nu$ from $B^0 \to D^{(*)} \ell\nu$ hierarchy.

FCC : Some words about guesstimation of the BF for unseen modes

- $B_s^0 \to K^{*0} D^{(*)} \tau \nu$ from analogy via phase space computation[7]:

$$BF(B_s^0 \to K^{*0} D^{(*)} \tau \nu) = BF(B_s^0 \to D_{s1} \mu \nu) \times \frac{PS(B_s^0 \to K^{*0} D^{(*)} \tau \nu)}{PS(B_s^0 \to D_{s1} \mu \nu)}$$

  where PS denotes the Phase Space computed numerricaly (three body decay hypothesis used conservatively) and $B_s^0 \to D_{s1} \mu \nu$ is a reference mode with a known BF.

- $B_s^0 \to K^{*0} D \tau \nu$ and $B_s^0 \to K^{*0} D^{*} \tau \nu$ w.r.t. $B_s^0 \to K^{*0} D^{(*)} \tau \nu$ from $B^0 \to D^{(*)} \ell \nu$ hierarchy.

FCC : some words about the choice of background to consider

- $B^0 \to K^{*0} D_s D_s$ with the two D_s deacying as $D_s \to \tau\nu$, $D_s \to \pi\pi\pi\pi^0$ and $D_s \to \pi\pi\pi\pi^0\pi^0$ already generated.
- $B^0 \to K^{*0} D_s^* D_s$ with the two D_s deacying as $D_s \to \tau\nu$ already generated.
- $B^0 \to K^{*0} D_s D_s$ with both $D_s \to \tau\nu$ and $D_s \to \pi\pi\pi\pi^0$ already generated.
- Construction of a "per track" efficiency by taking the square root of the reconstruction efficiency of the four first modes $\Rightarrow \epsilon(D_s \to \tau\nu)$, $\epsilon(D_s^* \to \tau\nu)$, $\epsilon(D_s \to \pi\pi\pi\pi^0)$ and $\epsilon(D_s \to \pi\pi\pi\pi^0\pi^0)$.
- Cross check : $\epsilon(D_s \to \tau\nu) \times \epsilon(D_s \to \pi\pi\pi\pi^0) \simeq \epsilon(B^0 \to K^{*0} D_s D_s, D_s \to \tau\nu, D_s \to \pi\pi\pi\pi^0)$.
- Construction of an $\epsilon(*) = \epsilon(D_s^* \to \tau\nu)/\epsilon(D_s \to \tau\nu)$.
- Computation of an estimated efficiency for the possible background from these per track efficiencies.
- Ranking of the backgrounds via $BF \times \epsilon$.
- Choice of the biggest one for each type of specific topology.

FCC : preselection

- Several kinematics variables has been save for each events (like momentum or intermediate mass).
- Among them several discriminatives variables have been found.
- The preselection has been built with these variables.
- The plot displays the result after preselection $\rightarrow$ the picture show a first improvement.
- The MVA can be trained against the backgrounds on the [5,5.6] GeV mass window.

Variable	Cut
$m^2_{2\pi_{min}}$ & $m^2_{2\pi_{max}}$	<0.3 & <0.5 GeV
p_{K^*}	$<$ 1GeV
$p_{3\pi}$	$<$ 1GeV
$p_{\pi_{max}}$	$<$ 0.25GeV
$p_{\pi_{min}}$	$<$ 0.2GeV
FD_B	$<$ 0.3mm
FD_τ	$>$ 4mm
$m_{3\pi}$	$<$ 0.750GeV
$m_{2\pi_{max}}$	$<$ 0.5GeV
$m_{2\pi_{min}}$	$>$ 1GeV

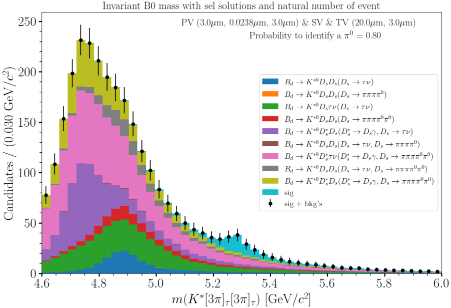

FCC : MVA

- Training dataset generated with signal and the collection of available backgrounds.
- The backgrounds are considered in natural proportion (after the preselection).
- 50/50 split train/validation.
- Previous variables are given as inputs as well as the reconstructed p_τ of each τ candidate.
- XGB parameters optimised on AUC.
- Overtraining plot in order to check the validity of the training $\rightarrow$ OK.
- Use of the MVA[vii] to perform the selection (cut at 0.5 on the BDT output).

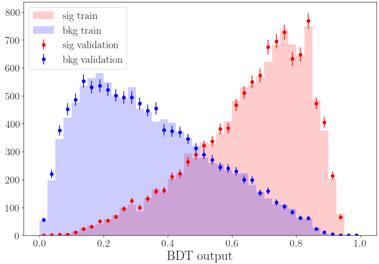

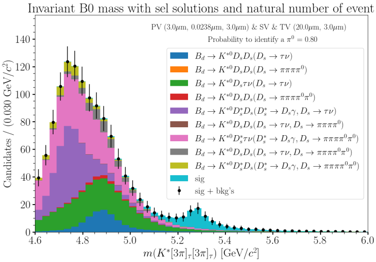

Tianqi Chen and Carlos Guestrin.
Xgboost: A scalable tree boosting system.
In *Proceedings of the 22nd acm sigkdd international conference on knowledge discovery and data mining*, pages 785–794, 2016.

Paul Langacker.
The physics of heavy z' gauge bosons.
Reviews of Modern Physics, 81(3):1199, 2009.

I Dorsner, S Fajfer, A Greljo, JF Kamenik, and N Kosnik.
Physics of leptoquarks in precision experiments and at particle colliders.
Physics Reports, 641:1–68, 2016.

JF Kamenik, S Monteil, A Semkiv, and L Vale Silva.
Lepton polarization asymmetries in rare semi-tauonic $b \to s$ b$\to$ s exclusive decays at fcc-ee.
The European Physical Journal C, 77(10):1–19, 2017.

BABAR Collaboration et al.
Search for b+-> k+ tau (+) tau (-) at the babar experiment.
Physical Review Letters, 2017, vol. 118, num. 3, p. 031802, 2017.

CERN.
2nd fcc-france workshop, jan 20-21, 2021.
https:...Physics.pdf.

Lingfeng Li and Tao Liu.
$b \to s\tau + \tau$- physics at future z factories.
Journal of High Energy Physics, 2021(6):1–31, 2021.

Torbjörn Sjöstrand, Stefan Ask, Jesper R Christiansen, Richard Corke, Nishita Desai, Philip Ilten, Stephen Mrenna, Stefan Prestel, Christine O Rasmussen, and Peter Z Skands.
An introduction to pythia 8.2.
Computer physics communications, 191:159–177, 2015.

Anders Ryd, David Lange, Natalia Kuznetsova, Sophie Versille, Marcello Rotondo, DP Kirkby, FK Wuerthwein, and A Ishikawa.
Evtgen: a monte carlo generator for b-physics.
BAD, 522:v6, 2005.

J De Favereau, Christophe Delaere, Pavel Demin, Andrea Giammanco, Vincent Lemaitre, Alexandre Mertens, Michele Selvaggi, Delphes 3 Collaboration, et al.
Delphes 3: a modular framework for fast simulation of a generic collider experiment.
Journal of High Energy Physics, 2014(2):57, 2014.

LHCb collaboration.
First observation of the $B^+ \to D_s^+ D_s^- K^+$ decay, 2022.